INFLUENCE OF SPECIMEN GEOMETRY AND LOADING MODE ON THE DAMAGE IN DUCTILE FAILURE

J. Arndt*, A. Sprock*, N. Schlüter*, D. Holland+ and W. Dahl*

Notched tensile bars and fracture mechanics specimens of two different structural steels are loaded up to initiation of stable crack growth. Finite Element calculations are carried out to determine the local stress and strain state of the damaged areas and the local failure curves. The influence of the local stress state on these curves is shown, discussed and compared with the global parameters of failure.

INTRODUCTION

Damage in ductile failure is characterized by void nucleation, growth and coalescense. Even at small plastic strains the inclusions are released from the ductile matrix and in that way cause the nucleation of voids, which grow with increasing load. Coalescense starts as soon as the damage reaches a maximum inside the material. If the damage maximum lies in front of a free surface a microcrack evolves between the void and the surface. Both mechanisms lead to a first microcrack growing with increasing load. At initiation the microcrack has a critical length. The length depends only on the material and is defined as l_c. Further crack growth weakens the cross section and leads to an increasing stress. Hence the initiation of a microcrack is a critical process for specimens and engineering components.

There are different criteria to explain the nucleation of voids: Some of them postulate a critical stress state at the interface of matrix and inclusion (1). Others postulate a critical strain level (2) or a critical combination of stresses and strains (3). For the void growth there are also different criteria. Each criterion contains the stress triaxiality $h = \sigma_m/\sigma_v$ which controls the void growth (4). The fraction of the void volume resulting from the void growth predominates the fraction resulting from void nucleation. So the criteria of void growth seem to be more important.

Different criteria are also given for the void coalescense similar to the void nucleation. Taking all above into account one can conclude that the variables local stress and local strain determine the process of ductile fracture. This led to the introduction of failure curves, which describe the local plastic strain ϵ_{vp}

* Institute for Ferrous Metallurgy, Technical University Aachen, FRG
+ Siempelkamp Giesserei GmbH & Co., Krefeld, FRG

as a function of the stress triaxiality at initiation (5,6). Every locus of the failure curve represents a critical combination at which crack initiation inside the material takes place.

INFLUENCES

The influences which determine the damage behaviour can be devided into external and internal factors (Fig. 1). The external factors are represented by the strain rate $\dot{\epsilon}$ and the temperature T. Both are kept constant in the experiments by working at a quasistatic strain rate and at room temperature. Furthermore there are the loading modes like bending and/or tension, the load level and the specimen geometry like specimen dimension and the flaw geometry. These factors influence the local stress and strain distribution and the damage behaviour of the materials.

The damage behaviour of the materials with different loadings is determined by their microstructure. These internal factors are the kind of structure, their volume fraction, shape, orientation and distribution. Most important in this context are less ductile inclusions in a ductile matrix. The inclusions were found to be non-metallic and mostly MnS-type in the steels under investigation.

RESULTS OF THE EXPERIMENTAL INVESTIGATIONS

The damage investigations were conducted on two structural steels FeE 690 and FeE 310. Notched tensile bars and three point bend specimen of both steels were tested. They were loaded up to initiation and afterwards the critical distance l_c was measured. The critical length l_c is defined by the distance between two coalescing microvoids if failure occurs inside the material. In case of initiation at the tip of a notch or of a crack the critical length l_c is given by the distance between a microvoid and the notched ground or the blunted crack tip, respectively. Fig. 2 illustrates both mechanisms schematically.

Notched Tensile Bars

The influence of the stress triaxiality and the plastic strain on the failure behaviour was examined on notched tensile bars of the geometry B8*40. In order to vary the stress state of the specimen, different notches were milled. Firstly the results of the steel FeE 690 are shown. The notch radius ρ is in the range of 0.5 to 4.0mm, the depth t is in the range of 0.5 to 1.5mm. Up to seven specimens of each geometry were tested. The first specimen of a series was loaded up to the steep drop of the load displacement curve, unloaded, cut longwise and prepared metallographically. If a microcrack was found in the polished microsection, the displacement of the next specimen was reduced and the specimen was examined. By using this method it was possible to determine the critical displacement at initiation exactly (7).

Finite Element Analysis with the FE-programme ABAQUS were carried out to determine the local stresses and strains at the locus of the crack

initiation. The stress triaxiality σ_m/σ_v and the equivalent plastic strain ϵ_{vp} are chosen to be the significant quantities. Figs. 3 and 4 show the distribution for different load levels. All specimens showed initiation in the centre of the tensile bar except for the specimens with the sharp notches where initiation occured close to the notched ground. The specimens with the mild notches have small gradients of stress triaxiality and plastic strain in the centre of the specimen whereas the specimens with the sharp notches have steep gradients close to the notched ground. For the specimen with the mild notches the determination of the critical values of stress triaxiality and plastic strain is insensitive for variing the critical distance l_c. In contrast to that the determination of the critical stress triaxiality and plastic strain of the specimens with sharp notches is very sensitive for varying the critical distance l_c because of the steep gradients. A critical distance l_c of 40μm influences the values of stress triaxiality and equivalent plastic strain at initiation very strongly.

The investigations on the steel FeE 310 were similar. The critical length was measured as 19μm. The failure curve is shown in Fig. 6. Obviously the failure curve of the FeE 690 is situated above the failure curve of the FeE 310. This means that crack initiation in the FeE 310 steel occurs at lower values of stress triaxiality and equivalent plastic strain. This is consistent with the lower toughness of this steel as measured earlier.

Three point bend specimen with fatigue crack

For the determination of the failure curve three point bend specimens of the dimension 13*26 with 20% side grooves were also tested (8). Side grooving provides an even crack front to keep the stress state constant all over the crack front. This leads to a simultaneous crack initiation along the crack front. In order to vary the stress and strain condition in front of the crack tip three point bend specimens with different a/W-ratios in the range of 0.1 to 0.5 were tested. Further experiments with three point bend specimens with an a/W-ratio of 0.8 showed no essential differences to the results of the specimens with an a/W-ratio of 0.5. The procedure for the exact determination of crack initiation point was similar to the one used for the notched tensile bars. The first specimen of a series was loaded until crack initiation was found by using the direct current potential drop method (DCPD). Then the specimen was heat tinted, broken in liquid nitrogen and the crack plane was examined to ensure stable crack growth using an optical microscope. The other specimens were loaded up to smaller displacements in order to approximate the critical displacement at initiation. FEA shows the local stress and strain state for all tested geometries at critical load (Figs. 7 and 8). Afterwards the critical length l_c was measured from tested specimens which had been prepared metallographically but were not broken in liquid nitrogen. Either the distance between the first void in the ligament and the blunted crack tip or the distance of the first part of a stable crack was measured. Fig. 9 shows the distribution of the measured critical lengths l_c. There is a good agreement between the critical lengths measured on the tensile bars and the three point bend specimens. Fig. 10 shows the failure curve of the three point bend specimens of the steel FeE 690. The failure curves

obtained from 3PB specimens and notched tensile bars are found to have a slight deviation. However, FeE 310 steel exhibits similar results.

DISCUSSION

A further study on the damaged areas demonstrates the essential differences in the load history of the notched tensile bars and the precracked three point bend specimens. Fig. 11 shows the load history of two different notched tensile bars. The specimen with the sharp notch reaches a high value of equivalent plastic strain and a low value of stress triaxiality. In this case initiation occurs close to the notch root. The specimen with the mild notch reaches a low value of equivalent plastic strain and a high value of stress triaxiality. In this case initiation occurs in the centre of the specimen. The figure indicates that the stress triaxiality is hardly changing with increasing plastic strain for both the mild notched specimen and the sharp notched specimen. As soon as the load condition at any locus in the ligament reaches the critical combination given by the failure curve, initiation occurs at this locus. The locus of initiation of all specimens corresponds with the locus determined in the experiment. The FEA of the load history indicates that the load of the initiation loci has never been exposed to a load condition given by the failure curve. Initiation occurs when the curve of the load history intersects the failure curve the first time.

Fig. 12 shows the local stress-strain state in the cross section of the ligament at initiation and the failure curve for the same specimens. The points of initiation are also marked. In the whole specimen there are no points having higher load conditions than the one at initiation. Hence the failure curve represents the failure locus of the notched tensile bars. All other loci reveal voids but no microcracks.

The load history in front of the crack tip of two three point bend specimens with different a/W-ratios is given in fig. 13. In contrast to the notched tensile bars, much higher values of stress triaxiality are reached in front of the crack tip at the beginning of the deformation. With increasing load and blunting of the crack tip the stress triaxiality is reduced even at low plastic strains. Initiation occurs at similar stress-strain states such as at the notched tensile bars. Fig. 14 shows the load history of several points right in front of the crack tip. Obviously the equivalent plastic strain at initiation increases with decreasing length of the fatigue precrack whereas the maximum stress triaxiality in the load history as well as the stress triaxiality at initiation decreases.

These considerations are exclusively restricted to a criterion of the local failure in ductile fracture. Hereafter global criteria are discussed. The J-integral at initiation J_i is such a failure criterion for fracture mechanics specimens. Experimental and numerical investigations have reported a geometry dependence of the J-integral, which particularly appears at different a/W-ratios (8). Fig. 15 shows J_i as a function of a/W-ratio. At small a/W-ratios the J-integral increases sharply. The enhanced toughness can be explained by the loss of stress triaxiality, which reduces the constraint against plastic flow and results in a large plastic deformation (9). A promising

parameter to explain the loss of constraint is the elastic T-stress(10). It is the second term in an elastic cracktip field and consists of an uniaxial tensile or compressive stress parallel to the crack flanks. Small a/W-ratios show negative T-stresses. They are compressive stresses and they reduce the stress triaxiality in front of the crack tip. Fig. 16 shows the J-integral J_i at initiation as a function of the T-stress which is normalized by the yield stress. The progress of the global J-T-failure curve is similar to the one of the local failure curve. The J-integral at initiation increases if T-stresses become negative, because of decreasing a/W-ratio.

If the J-integral which is used to indicate the strain density energy on the crack tip, and the T-stress which correlates with the stress triaxiality are replaced by the local quantities ϵ_{vp} and σ_m/σ_v it follows that the global failure curve results in the same local failure curve qualitatively.

CONCLUSIONS

Local failure curves describe the damage behaviour of different specimen like notched tensile bars and precracked three point bend specimen with only a small deviation. Both types of specimen have different load histories. But the load history does not seem to severly affect the damage curve. Further investigations of the load history confirm that the locus of initiation has no higher critical combination of stress triaxiality and equivalent plastic strain than given by the failure curve before initiation. Investigations of the remaining parts of the specimen revealed that the load at the initiation locus has always been the highest. Replacing the local stress triaxiality and the local strain by the global parameters of T-stress and J-integral leads to global failure curves which describe the failure behaviour of the whole specimen. Local and global failure curves show similar behaviour.

LIST OF SYMBOLS

a_0 = fatigue crack length [mm]

h = stress triaxiality [1]

J_i = J-integral at initiation [kJ/m^2]

l_c = critical length [mm]

t = notch depth [mm]

T = temperature [K]

T = T-stress [MPa]

W = width of specimen [mm]

$\dot{\epsilon}$ = strain rate [1/s]

ϵ_{vp} = equivalent plastic strain [1]

ρ = notch radius [mm]

$\sigma_{1,2,3}$ = maximum normal stress [MPa]

σ_m = average normal stress [MPa]

σ_v = equivalent stress by von Mises [MPa]

ACKNOLEDGEMENTS

The authors wish to express their apprecation to the "Deutsche Forschungsgemeinschaft (DFG)" for their financal support of the project Da 85-61. The ABAQUS finite element programme was made available under academic license from Hibbitt, Karlsson and Sorensen, Inc., Pawtucket, R.I., USA.

REFERENCES

(1) Beremin, F.M., Metallurgical Transactions A, Vol.12 A, 1981, pp. 723-731

(2) Chu, C.C. and Needleman, A., Journal of Engineering Materials and Technology, Vol. 112, 1980, pp. 249-256

(3) Beremin, F.M., Proceedings ICF 5, Cannes, France, 1981, pp. 809-816

(4) Seidenfuß, M., Untersuchungen zur Beschreibung des Versagens verhaltens mit Hilfe von Schädigungsmodellen am Beispiel des Werk stoffes 20 MnMoNi 5 5, Techn.-wiss. Ber. MPA Stuttgart, 1992

(5) Hancock, J.W. and Mackenzie, A.C., J. Mech. Phys. Solids 24, 1976, pp. 147-169

(6) Kong, X.M., Holland, D., Schlüter, N., Arndt, J. and Dahl, W., Proceedings ECF 9, Varna, Bulgaria, 1992, pp. 677-684

(7) Holland, D., Schlüter, N., Kong, X.M., Arndt, J. and Dahl, W., Tagungsband Abschlußkolloquium DFG Schwerpunktprogramm "Schädigungsfrüherkennung" des DVM, 1992, pp. 21-39

(8) Holland, D., "Einfluß des Spannungszustandes auf die Vorgänge beim Gleitbruch von Baustählen, Berichte aus dem Institut für Eisenhüttenkunde, Aachen, 1992

(9) Al-Ani, A.M. and Hancock, J.W., J. Mech. Phys. Solids, Vol. 39, No. 1, 1991, pp. 23-43

(10) Sprock, A., Shallow Crack Fracture Mechanics, Toughness Tests and Applications, Cambride, UK, 1992

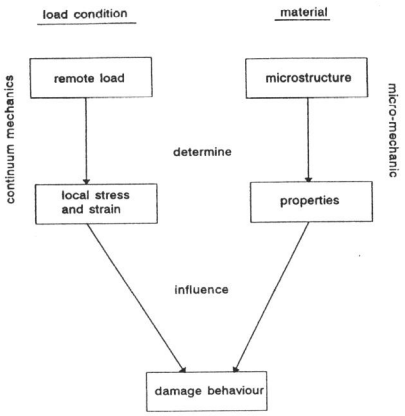

Figure 1. Influences on the damage behaviour

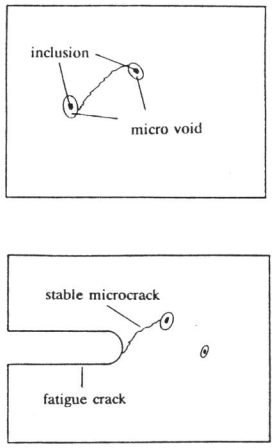

Figure 2. Critical distance l_c

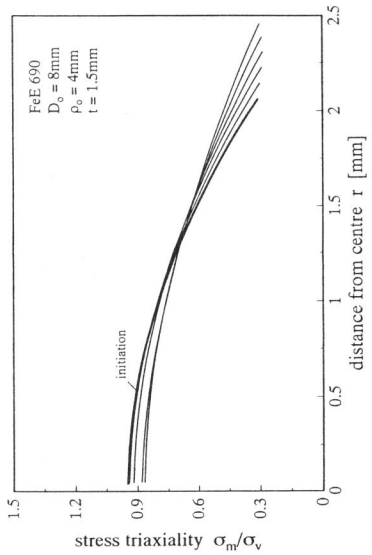

Figure 3. Stress triaxiality of a mild notched tensile bar

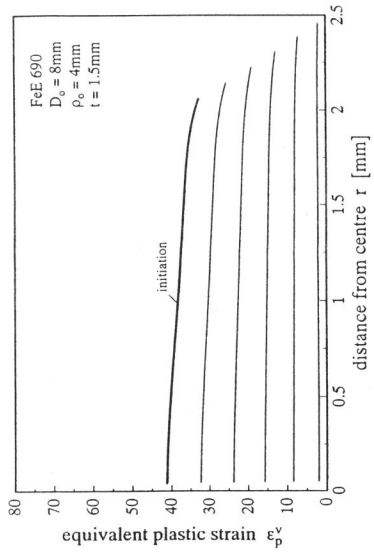

Figure 4. Equivalent plastic strain of a mild notched tensile bar

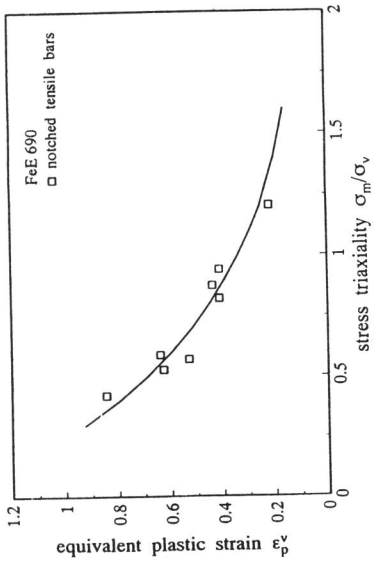

Figure 5. Damage curve of the steel grade FeE 690 (tensile bars)

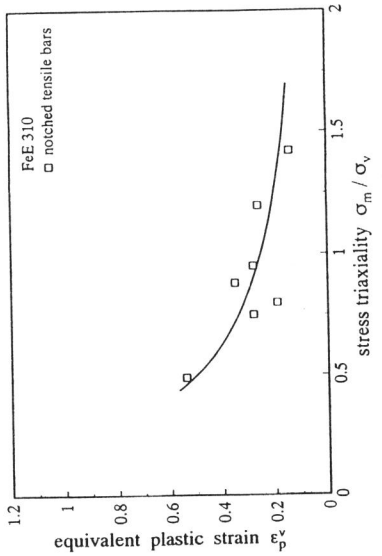

Figure 6. Damage curve of the steel grade FeE 310 (tensile bars)

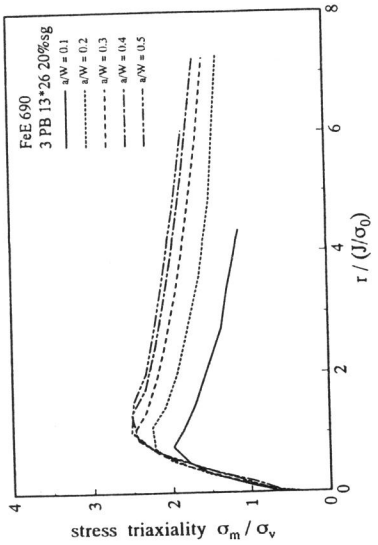

Figure 7. Stress triaxiality at initiation in the ligament

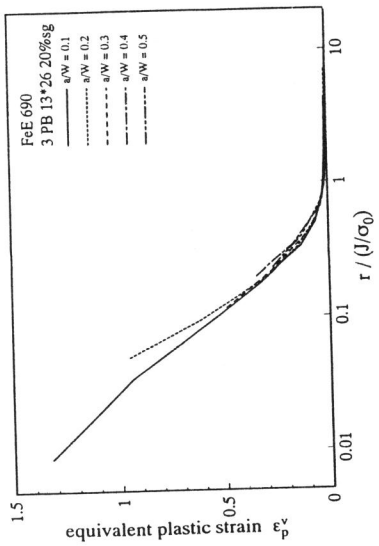

Figure 8. Equivalent plastic strain at initiation in the ligament

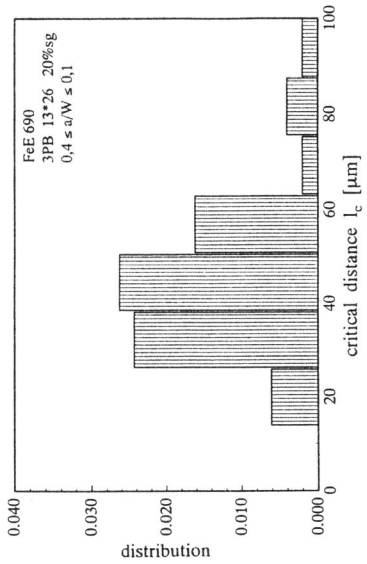

Figure 9. Critical distance l_c

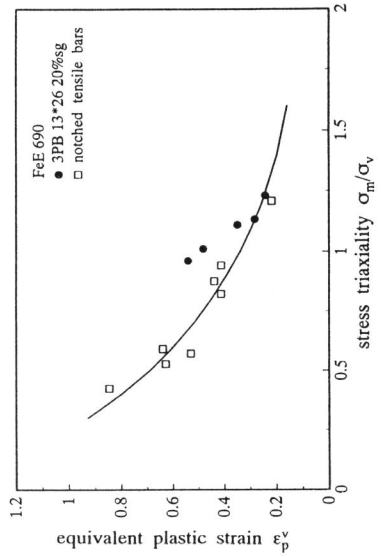

Figure 10. Damage curve of the steel FeE 690 (3PB 13*26 20%sg)

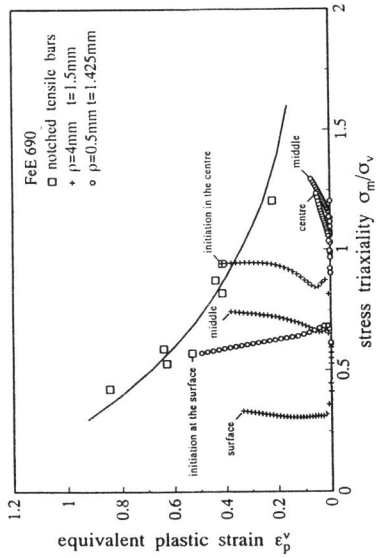

Figure 11. Load history of two different tensile bars

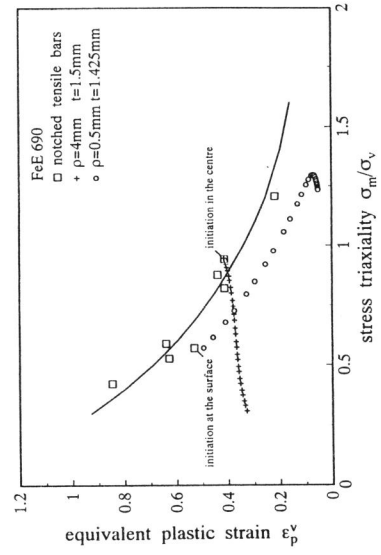

Figure 12. Load condition of two different tensile bars

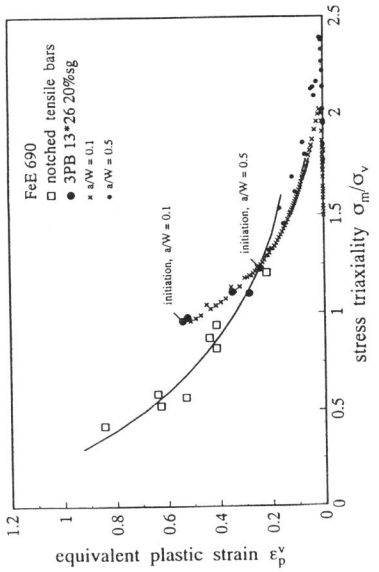

Figure 13. Load history of two different 3PB 13*26 20%sg

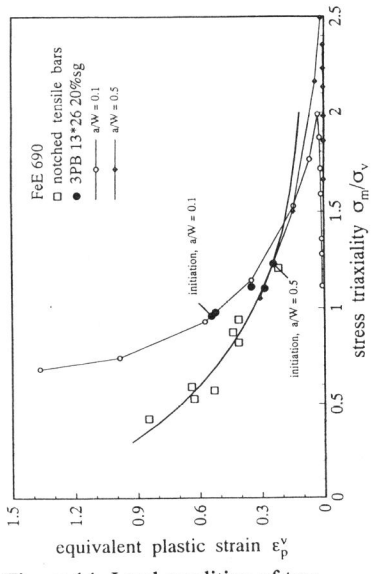

Figure 14. Load condition of two different 3PB 13*26 20%sg

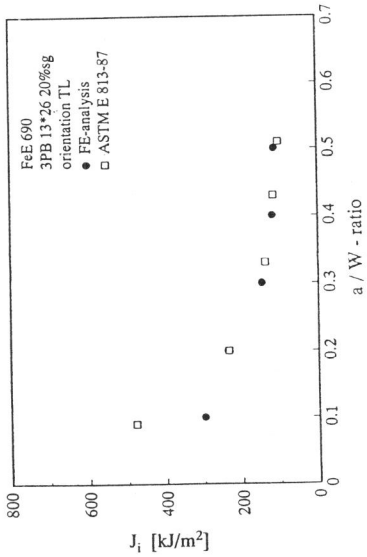

Figure 15. J-integral J_i at initiation for different crack depths

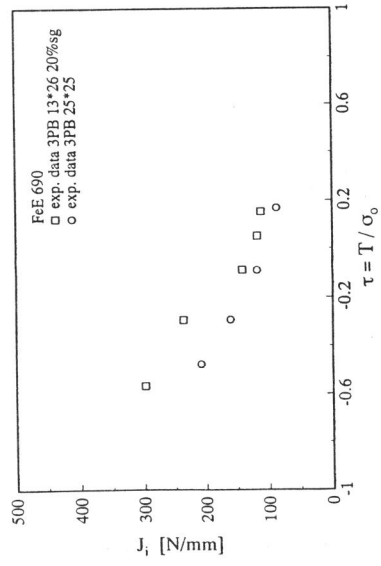

Figure 16. J-integral J_i at initiation for different T-stresses